ACS APPLIED MATERIALS & INTERFACES

LETTER

www.acsami.org

Study of Antisite Defects in Hydrothermally Prepared $LiFePO_4$ by in Situ X-ray Diffraction

Jiajun Chen* and Jason Graetz

Energy Science and Technology Department, Brookhaven National Laboratory, Upton, New York 11973, United States

Supporting Information

ABSTRACT: Hydrothermal synthesis has proven to be a cost-effective, energy-efficient approach for the manufacture of lithium iron phosphate ($LiFePO_4$) and its related materials. However, hydrothermally prepared $LiFePO_4$ typically suffers from antisite defects, where some of the iron resides on lithium sites and restricts lithium-ion mobility. A post-heat-treatment temperature of around 700 °C is generally used to eliminate cation disorder, but little is known about these antisite defects or their concentration as a function of the post-heat-treatment temperature. In this study, time-resolved, synchrotron X-ray diffraction reveals that antisite defects are completely eliminated above 500 °C, suggesting that the electrochemical performance may be significantly enhanced by a milder postsynthesis heat treatment. The preliminary electrochemical results show a significant enhancement in the electrochemical capacity with the defect-free material, with the specific capacity increasing by approximately 60% at a C/20 rate.

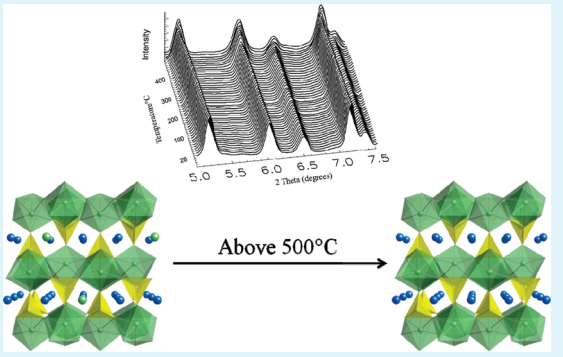

KEYWORDS: hydrothermal, cation disorder, lithium iron phosphate, in situ X-ray diffraction, battery cathode

Inspired by Goodenough et al.'s pioneering work,[1] olivine-phase lithium iron phosphate has been extensively studied as a promising cathode material over the past decade. This material has a high specific capacity, excellent thermal stability, and stable cyclability and appears to be one of the more attractive cathodes currently being considered for electric and hybrid-electric vehicle batteries.

$LiFePO_4$ adopts an olivine structure with a *Pnma* space group where lithium is contained within the tunnels of interconnected FeO_6 octahedra and PO_4 tetrahedra. The *Pnma* structure is stable over the full range of lithium concentrations ($0 \leq x \leq 1$), and therefore all of the lithium ions can be utilized in the electrochemical reaction, unlike in layered metal oxides, in which only about half of the lithium can be removed from the structure. During electrochemical cycling, the structure undergoes a volume change of only about 6.5% between lithiated $LiFePO_4$ and delithiated $FePO_4$, and therefore the material does not suffer significantly from particle decrepitation. Although the intrinsic conductivity of this material is low, it has been increased substantially by the addition of carbon coatings.

A key hurdle for the widespread commercialization of this material is the development of an economical manufacturing process. A low-temperature, soft-chemistry route, such as hydrothermal synthesis, offers a low-cost and efficient process for the manufacture of these electrode materials. However, it has been found that the site mixing of the cations (e.g., lithium and iron) is a potential problem with materials synthesized by this method,[2] and these types of crystallographic defects are well-known in intercalation compounds. One example is titanium disulfide, which has a perfect layered structure,[3] and the weak van der Waals force between the layers allows fast lithium intercalation and diffusion. However, the titanium atoms can occupy sites in the lithium layer when the synthesis conditions are not optimum. Disordered titanium in the structure severely impedes the lithium-ion diffusion and reduces the electrochemical performance of TiS_2; similar cases were also found in layered oxides.[4]

A key challenge with the *Pnma* structure is that lithium motion occurs through one-dimensional (1D) channels (along the *b* axis) and is unable to cross between channels because of a high activation barrier.[5] Unlike the two-dimensional lithium diffusion that occurs in the layered metal oxides, the ions in $LiFePO_4$ are restricted and cannot move around blocked sites. Antisite defects (e.g., iron on lithium sites) are a critical problem for lithium diffusion because a single blocked ion in the channel prevents lithium-ion transport into that channel.

The octahedrally coordinated cations, lithium and iron, in the naturally occurring mineral triphylite, are completely ordered between the M1 and M2 sites. However, $LiFePO_4$ synthesized at low temperature (120 °C) was shown to have almost 7% iron occupancy on the lithium sites.[6] In this case, the reactivity of the material was significantly reduced, reacting with only a small amount of butyllithium and not at all with bromine. The electrochemical capacity of these samples measured at low current densities was also small.[7] More recent research has shown that the hydrothermal synthesis temperature is a critical factor in the formation of antisite defects in olivine metal phosphates.[8] A higher synthesis temperature or a longer heat treatment of the as-synthesized material is believed

Received: February 1, 2011
Accepted: April 28, 2011
Published: April 28, 2011

to be effective at reducing the cation disorder. Recently, studies have shown that a synthesis temperature of around 700 °C is sufficient to completely eliminate the cation disorder;[3,7] however, the exact temperature at which this transition occurs is unknown.

There is currently a need to quantify the concentration of antisite defects in $LiFePO_4$ as a function of the synthesis or post-heat-treatment temperature. Theoretical studies have shown that antisite defects are likely in $LiFePO_4$;[9] however, the concentration of such defects has not been determined experimentally. A number of ex situ investigations of cation disorder have been reported for both layered oxides and metal phosphates,[10,11] and measurements of iron and lithium site defects in hydrothermally prepared $LiFePO_4$ were previously studied by Cu Kα powder X-ray diffraction (XRD). However, these data were insufficient to quantify the antisite defect concentration. A better understanding of the correlation between the synthesis conditions, crystallization processes, and properties requires real-time characterization. Previous studies failed to provide the real-time antisite defect concentration during post heat treatment. Here we report the measurement of the concentration of antisite defects as a function of the temperature by in situ high-resolution XRD to shed light on the defect elimination process during heat treatment. In situ observations of antisite defect elimination or creation are necessary to understand the defect formation and ultimately enhance the lithium-ion mobility in these materials by manipulating point defects.

A structural investigation of hydrothermally synthesized $LiFePO_4$ was carried out by high-resolution synchrotron radiation at Beamline X7B of the National Synchrotron Light Source (NSLS) at Brookhaven National Laboratory (BNL). $LiFePO_4$ used in this study consisted of micrometer-sized particles prepared by the conventional hydrothermal synthesis. The particles were diamond-shaped platelets of 1−2 μm on edge. High-resolution synchrotron XRD was acquired over a wide in 2θ range (0.01−55°) using an X-ray wavelength of 0.3184 Å for both the ex situ and in situ samples. Approximately 4391 reflections were recorded, significantly larger than the number of peaks typically recorded on a laboratory Cu Kα powder X-ray diffractometer. The ex situ data were fit using GSAS Reitveld refinement over a 2θ range of 3−55° with a Chebyshev polynomial function and 20 coefficients for the background. The full XRD patterns were perfectly indexed as orthorhombic with a *Pnma* space group, and no impurity peaks were observed (an example is shown in Figure 1). All refinements from the ex situ samples terminated at reliability values of R_{wp} = 2.3% and R_p = 1.7%. A similar refinement was used for the in situ (variable-temperature) data, but the fit was restricted to a 2θ range of 3−25°, which included 482 reflections. As expected, no phase transformations were observed during heating because the material was heated under an inert atmosphere. All refinements from the in situ samples terminated at reliability values of around R_{wp} = 2.6% and R_p = 1.9%.

In the olivine structure of $LiFePO_4$, both iron and lithium ions occupy octahedral sites, while phosphorus is in a tetrahedral site with a hexagonal close-packed structure. The distorted FeO_6 octahedron and PO_4 tetrahedron form tunnels through the structure (where the lithium resides), which restricts the lithium to 1D movement along the *b* axis, as illustrated in the inset of Figure 1.

Chemical analysis of the as-synthesized $LiFePO_4$ (before heat treatment) using inductively coupled plasma optical emission spectrometry (ICP-OES) revealed a significantly iron-rich sample with Fe:Li = 1.49:1. This is consistent with previous reports by other groups, who reported a Fe:Li molar ratio of 1.41 in $LiFePO_4$[10] or a Mn:Li molar ratio of 1.31 in $LiMnPO_4$.[11] The high iron

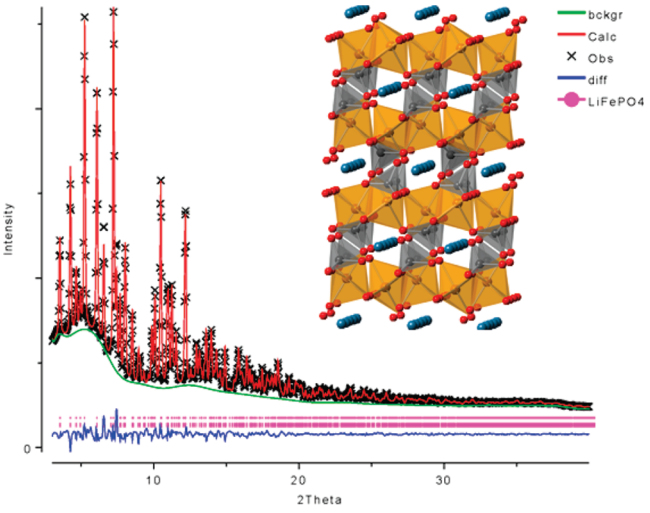

Figure 1. Example of high-resolution synchrotron XRD and Rietveld refinement patterns from hydrothermally prepared $LiFePO_4$. The differences between the observed and calculated intensities are plotted. The inset shows the atomic structure of $LiFePO_4$, revealing the lithium tunnels.

content (determined by the ICP analysis) suggests that it is unlikely that all of the excess iron is incorporated into the structure but rather that some of it likely resides on the surface. It is possible that some of the excess iron diffuses to the surface of the particles, where it forms a second phase (e.g., Fe_2O_3), which is not detected by XRD. Similar amorphous surface impurities have been reported by Shiraishi et al.[12,13]

Two crystallographic models are most likely for cation disorder in these samples, a lithium−iron mixing model ($Li_{1-y}Fe_y$-$[Li_yFe_{1-y}]PO_4$) and an iron-rich model ($Li_{1-2y}Fe_yFePO_4$). Previous single-crystal studies have shown that the iron-rich model shows the best structural solution for hydrothermally prepared lithium iron phosphate.[2] Similar results were obtained for hydrothermally prepared manganese phosphate.[11] We performed refinements using both models and found the best fits with the iron-rich system, consistent with ICP-OES results, and this model (iron-rich) was used for refinements of the site occupancy and to investigate the cation distribution. The iron (M2) 4c site occupancy was restricted to unity. Several trial refinements were carried out with the shared lithium site (4a) occupancy initially set to different values (i.e., 0.95 and 0.9) to ensure the consistency of each refinement. The refinements were consistently refined to similar values, suggesting that the results are reliable.

As-prepared, hydrothermally synthesized $LiFePO_4$ (no heating) was determined to have around 6.7(2)% cation disorder, with the lithium octahedral M1 site (4a) containing 6.7(2)% iron. The structural formula is $Li_{0.866}Fe_{0.067}FePO_4$, with lithium vacancies for the charge compensation to high-valent iron(II). Previous studies of $LiFePO_4$ prepared by low-temperature synthesis have found excess iron on lithium sites in the range of 5−10%,[6,14] which is consistent with our result of 6.7%. On the basis of the ICP results and the stoichiometry of $Li_{0.866}Fe_{0.067}FePO_4$, determined from Rietveld refinement, we find that antisite defects account for about half of the excess iron in the system. The remaining excess iron is likely present as an amorphous phase on the surface.

The measured lattice constants from $LiFePO_4$ before heat treatment were *a* = 10.3658(6) Å, *b* = 6.0037(3) Å, and *c* = 4.7124(3) Å with a cell volume V = 293.27(2) Å^3, which is in

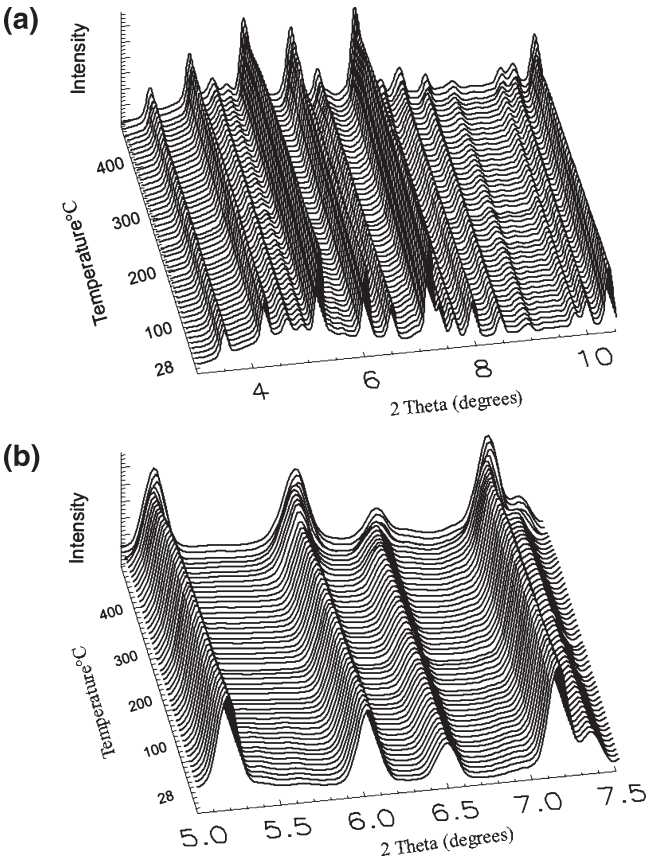

Figure 2. (a) In situ high-resolution synchrotron XRD pattern from hydrothermally synthesized $LiFePO_4$ during heat treatment. (b) Expanded region of the XRD pattern (2θ 5−7.5°) showing a shift of the peak position.

agreement with previous reports for the slightly expanded cell dimension.[15] The standard cell volume[16] for defect-free $LiFePO_4$ is typically 291.4 Å^3. The hydrothermally prepared sample used in this study had a defect concentration similar to that of $LiFePO_4$ single crystals ($Li_{0.94}Fe_{0.03}FePO_4$) formed hydrothermally at 180 °C for 3 h, as reported by Chen et al.,[2] but many more defects than materials synthesized at the same temperature for longer time. The organic acid and synthesis dwelling time were found to impact the concentration of defects, which will be reported elsewhere.

A series of powder patterns were recorded over a temperature range between 28 and 500 °C using a ramping rate of 2.6 °C/min. At the end of the ramp, the temperature was held constant at 500 °C for 10 min. In situ high-resolution synchrotron XRD patterns from hydrothermally synthesized $LiFePO_4$ during heating are shown in Figure 2. The anisotropic variation of the unit cell parameters is shown in Figure 3. Upon heating to 450 °C, all Bragg peaks shift to lower 2θ angles, indicating an increase in the unit cell parameters due to thermal expansion. The *a* lattice constant was initially 10.3658(6) Å and increased up to 10.3954(9) Å at 443 °C, while the *b* lattice constant was initially 6.0037(3) Å and gradually increased up to 6.0371(5) Å at a temperature of 453 °C. In contrast, the *c* lattice constant continually increased from 4.7124(3) to 4.7501(6) Å until the temperature reached 500 °C. The cell volume reached the highest value at 452 °C with cell dimensions of a = 10.3934(9) Å, b = 6.0371(5) Å, and c = 4.7455(4) Å and a cell volume of 297.84(4) Å^3.

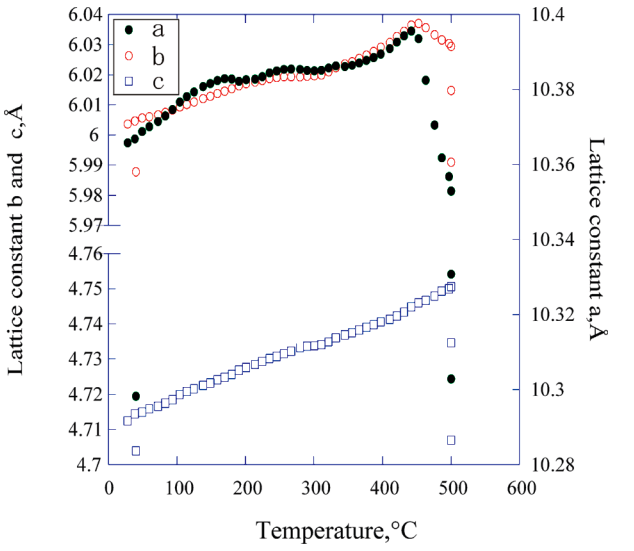

Figure 3. Lattice parameters *a*, *b*, and *c* change as a function of the temperature.

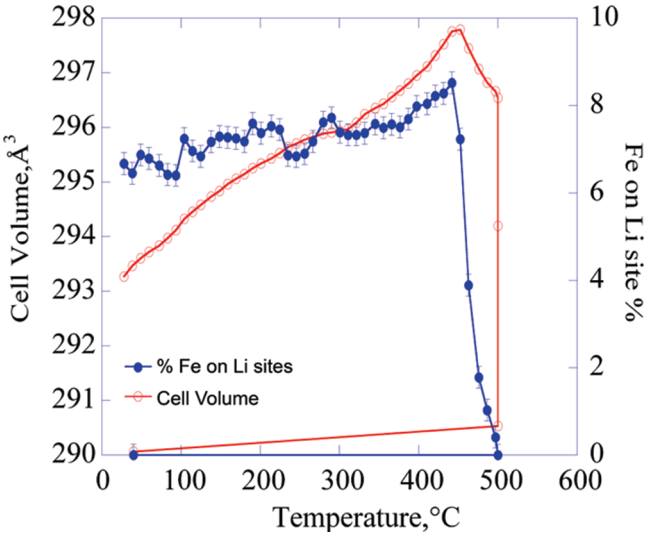

Figure 4. Unit cell volume and the concentration (percent) of iron on lithium sites as a function of temperature.

The concentration of iron on lithium sites increases slightly with an increase in the temperature up to 442 °C, as shown in Figure 4. At 442 °C, approximately 8.5(2)% of the iron remained on the lithium sites. The onset of cation ordering occurred around 450 °C. At this transition temperature, all crystallographic reflections shift toward a higher 2θ angle, suggesting a decrease in the unit cell dimensions. The number of antisite defects abruptly dropped to essentially zero when the temperature reached around 500 °C. The cell volume decreased to 290.46(4) Å^3 after the temperature was held constant at 500 °C for 10 min. As the sample cooled to about room temperature (28 °C), the cell volume quickly decreased to 289.97(5) A^3. All of the standard deviation (σ) values for the refined site occupancies given by GSAS Expgui software are in the output data files (see the Supporting Information). The average of the refined atomic occupancy standard deviations is around 0.2%.

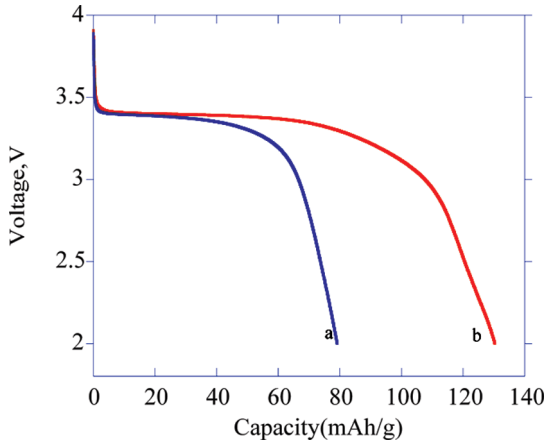

Figure 5. Electrochemical cycling discharge profiles of (a) $LiFePO_4$ before heat treatment and (b) after 500 °C heat treatment.

After heat treatment, the sample was resealed in a new quartz capillary, and another XRD pattern was acquired. $LiFePO_4$ exhibited a reduced lattice parameter at room temperature, with lattice constants a = 10.303(1) Å, b = 5.987(1) Å, and c = 4.670(1) Å and a cell volume of 289.87(5) Å^3. The reliability factors for this fit were R_{wp} = 2.3% and R_p = 1.8%. The observed decrease in the cell volume is in good agreement with recent report by Julien et al.[14,17] For micrometer-sized $LiFePO_4$, a unit cell volume of around 290−291.4 Å^3 is believed to be a good measure of complete cation order (no iron on lithium sites), which is consistent with our results from hydrothermally prepared samples after heat treatment.

At temperatures above 450 °C, the excess iron leaves the lithium sites. Although it is not clear from these data exactly where this excess iron goes, it does not seem to be incorporated into the structure and accommodated by other sites. It is possible that the excess iron diffuses to the surface of the particles, where it forms a second phase (e.g., Fe_2O_3). If this is the case, this other phase is composed of particles that are amorphous or too small to be detected by synchrotron XRD. The location of the excess iron after heat treatment is the subject of an ongoing investigation.

It is well-known that lithium-ion transport in $LiFePO_4$ occurs through the channels along the b direction[18] and the substitution of even a small amount of Fe atoms onto Li sites blocks the channels and impedes lithium-ion transport. Complete lithiation or delithiation of disordered $LiFePO_4$ requires migration of point defects, which is a significantly slower step. Thus, the overall lithium-ion mobility and reactivity of the material is greatly reduced by iron disorder, as reported by Whittingham et al.[19] The elimination of iron disorder upon heat treatment allows unimpeded lithium-ion transport along the b direction and is essential to achieving the best possible electrochemical performance from hydrothermally prepared $LiFePO_4$. As shown in Figure 5, we carried out a preliminary electrochemical study on $LiFePO_4$ before and after heat treatment at 500 °C. The results show significant improvement in the performance of the defect-free material, with the specific capacity increasing from 80 to 130 mAh/g at a rate of C/20. This result confirms that the presence of antisite defects (specifically, iron on lithium sites) limits lithium diffusion and reduces the electrochemical performance of the material. In order to test the effect of antisite defects on the electrochemical performance, no conductive surface carbon coating was applied, which requires higher temperature annealing (above 500 °C). Therefore, the capacity of the defect-free material is slightly below some of the best results from hydrothermally prepared $LiFePO_4$ published previously.[8]

In conclusion, we investigated the concentration of antisite defects in hydrothermally prepared $LiFePO_4$ as a function of the temperature by in situ high-resolution XRD. The amount of cation disorder was reduced as the temperature of the heat treatment was increased. The antisite defects were completely eliminated at ∼500 °C, significantly lower than the previously reported value of 700 °C. This suggests the postsynthesis heat treatment in an inert atmosphere (i.e., helium) is effective at reducing iron and lithium exchange. Our results also demonstrate that intrinsic structural defects in cathode materials can be monitored by in situ high-resolution synchrotron XRD. High-resolution synchrotron XRD not only is a method for measuring lattice constants but also is useful for accurately determining the site occupancy, which is critically important in cathodes with tunnel or layered structures where lithium-ion transport is often restricted by a small amount of disorder.

■ ASSOCIATED CONTENT

Ⓢ Supporting Information. Details for the experimental method of synthesis and characterization and electrochemical measurements, Rietveld refinement fitting procedure, table of representative refined atomic coordinates, atomic displacement parameters, and site occupancies, and crystallographic data files containing all refined atomic coordinates, atomic displacement parameters, and site occupancies of the in situ experiment from 28 to 500 °C. This material is available free of charge via the Internet at http://pubs.acs.org.

■ AUTHOR INFORMATION

Corresponding Author

*E-mail: jjchen@bnl.gov. Fax: 631-344-7905. Phone: 631-344-2479.

■ ACKNOWLEDGMENT

This work was supported by the U.S. Department of Energy (DOE) under Contract DE-AC02-98CH10886 with funding from Laboratory Directed Research and Development at BNL. Use of the NSLS at BNL was supported by the U.S. DOE, Office of Basic Energy Sciences (Grant DE-AC02-98CH10886). The authors are very grateful to Dr. Jonathan Hanson and Dr. Rui Si for fruitful discussion and technical support at NSLS Beamline X7B.

■ REFERENCES

(1) Padhi, A. K.; Nanjundaswamy, K. S.; Goodenough, J. B. *J. Electrochem. Soc.* **1997**, *144* (4), 1188–1194.

(2) Chen, J. J.; Vacchio, M. J.; Wang, S. J.; Chernova, N.; Zavalij, P. Y.; Whittingham, M. S. *Solid State Ionics* **2008**, *178* (31−32), 1676–1693.

(3) Whittingham, M. S. *Chem. Rev.* **2004**, *104* (10), 4271–4301.

(4) Lu, Z. H.; Beaulieu, L. Y.; Donaberger, R. A.; Thomas, C. L.; Dahn, J. R. *J. Electrochem. Soc.* **2002**, *149* (6), A778–A791.

(5) Morgan, D.; Van der Ven, A.; Ceder, G. *Electrochem. Solid-State Lett.* **2004**, *7* (2), A30–A32.

(6) Yang, S. F.; Zavalij, P. Y.; Whittingham, M. S. *Electrochem. Commun.* **2001**, *3* (9), 505–508.

(7) Yang, S. F.; Song, Y. N.; Ngala, K.; Zavalij, P. Y.; Whittingham, M. S. *J. Power Sources* **2003**, *119*, 239–246.

(8) Chen, J. J.; Whittingham, M. S. *Electrochem. Commun.* **2006**, *8* (5), 855–858.
(9) Islam, M. S.; Driscoll, D. J.; Fisher, C. A. J.; Slater, P. R. *Chem. Mater.* **2005**, *17* (20), 5085–5092.
(10) Liu, J. L.; Jiang, R. R.; Wang, X. Y.; Huang, T.; Yu, A. S. *J. Power Sources* **2009**, *194* (1), 536–540.
(11) Fang, H. S.; Pan, Z. Y.; Li, L. P.; Yang, Y.; Yan, G. F.; Li, G. S.; Wei, S. Q. *Electrochem. Commun.* **2008**, *10* (7), 1071–1073.
(12) Shiraishi, K.; Dokko, K.; Kanamura, K. *J. Power Sources* **2005**, *146* (1−2), 555–558.
(13) Dokko, K.; Shiraishi, K.; Kanamuraa, K. *J. Electrochem. Soc.* **2005**, *152* (11), A2199–A2202.
(14) Jozwiak, P.; Garbarczyk, J.; Gendron, F.; Mauger, A.; Julien, C. M. *J. Non-Cryst. Solids* **2008**, *354* (17), 1915–1925.
(15) Chen, J.; Wang, S.; Whittingham, M. S. *J. Power Sources* **2007**, *174* (2), 442–448.
(16) Streltsov, V. A.; Belokoneva, E. L.; Tsirelson, V. G.; Hansen, N. K. *Acta Crystallogr., Sect. B* **1993**, *49*, 147–153.
(17) Axmann, P.; Stinner, C.; Wohlfahrt-Mehrens, M.; Mauger, A.; Gendron, F.; Julien, C. M. *Chem. Mater.* **2009**, *21* (8), 1636–1644.
(18) Nishimura, S.; Kobayashi, G.; Ohoyama, K.; Kanno, R.; Yashima, M.; Yamada, A. *Nat. Mater.* **2008**, *7* (9), 707–711.
(19) Yang, S. F.; Song, Y. N.; Zavalij, P. Y.; Whittingham, M. S. *Electrochem. Commun.* **2002**, *4* (3), 239–244.